

The Investigation of a Unbalanced Barrel Pitching System's Characteristics Degradation and Compensation under Gradual Erosion Behavior

Yuanbo CHU*, Yunxia XIA**

*School of Photoelectric Engineering, Xi'an Technological University, Xi'an, 710021, China,
E-mail: chuyuanbo528@163.com

**Institute of Optics and Electronics, Chinese Academy of Science, Chengdu 610209, China,

**Key Laboratory of Optical Engineering, Chinese Academy of Sciences, Chengdu 610209, China
E-mail: xiayunxia@ioe.ac.cn (Corresponding Author)

<https://doi.org/10.5755/j02.mech.31873>

1. Introduction

The barrel stabilizer, also known as barrel control system, can make the barrel free from the influence of carrier pitching and steering, and ensure the firing of tank barrel during traveling shown as Fig.1. It can also control the position of the barrel in the vertical and horizontal direction, and implement rapid barrel adjusting and accurate aiming [1-2]. Because of the advantages of large power weight ratio, fast response, high control accuracy and strong load resistance rigidity, the electro-hydraulic servo control system are more adopted for barrel's vertical stability and rotation [3]. However, the electro-hydraulic servo systems usually have many uncertainties, such as complex external interference, unmodeled leakage, load mass change, oil elastic

modulus change and so on, which seriously restrict the reaction speed and control accuracy of the control system [4-6]. In addition, the core of the barrel pitching servo control system, the high precision jet pipe servo valve, belongs to a typical electro-mechanical coupling system [7-8]. The gradual wear behavior such as erosion during service will cause the irreversible change of the core parameters [9-10], which will degrade the performance of the servo valve and greatly aggravate the difficulty of barrel pitching control, which will lead to the reduction of the hit rate of barrel weapons and even the end of their service life. Therefore, the research on the performance degradation and effective compensation control of unbalanced barrel pitching servo system under the condition of erosion is a major strategic issue related to safety and stability.

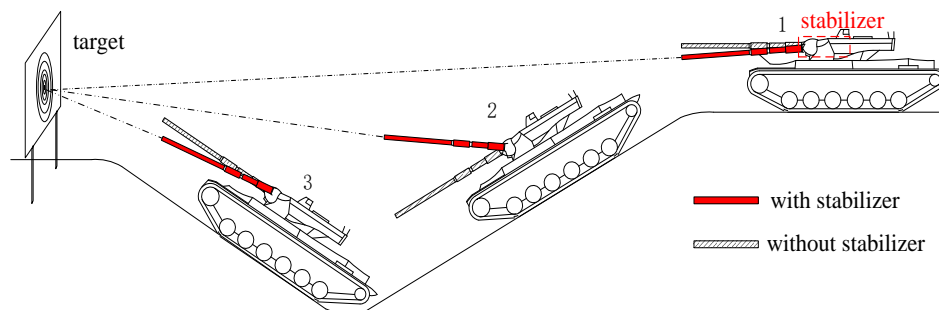


Fig. 1 Barrel's vertical pitching motion with and without stabilizer

The performance of unbalanced barrel pitching system has been studied for a long time. Lots of researches have been carried out in academic and engineering circles, the results show that unbalanced torque is an important reason for the deterioration of system control performance. If the center of barrel's gravity does not coincide with the rotation center, it will produce a non-equilibrium weight torque, which will change continuously with the rotation of the barrel and seriously deteriorate the positioning control performance of the barrel. At present, the methods of balancing such unbalance torque can be summarized as mass balance, balancing machine balance and adding driving source balance. Among them, mass balance and balancing machine balance are difficult to be popularized and applied because they cannot meet the requirements of system lightweight and compactness. Researchers of Nanjing University of technology [11-12] proposed a new electro-hydraulic servo system to balance and position the unbalanced barrel,

and use the balance chamber of three chamber hydraulic cylinder to actively compensate the unbalanced force of the system. At the same time, the two driving cavities are used for barrel positioning and interference suppression, and the system control is carried out by using the strategies of neural network active disturbance rejection control. This kind of method can realize the rapid stability and accurate control of large-diameter unbalanced barrel servo system.

However, the existing research on barrel pitching control does not involve the impact of erosion. The unbalanced barrel stability system involves many disciplines such as machinery, electrical, hydraulic and control, and the gradual erosion behavior of jet pipe servo valve in the system is very common such as Figs. 2 and 3. With the extension of service time, erosion will induce the irreversible deterioration of the core parameters, cause the degradation of barrel control performance, and seriously affect the hit probability and service reliability of barrel weapons. Early researches

about the electro-hydraulic servo system are more experimental method. Because the characteristics of which is long life, high reliability and complex structure, the experimental method has the disadvantages of long cycle, high cost and low accuracy. The development of computer and related theories makes it possible for its performance simulation, through the simulation, it is found that the gradual loss behavior causes the irreversible change of the core parameters, and the "software servo" compensation control of this kind of system can be completed with the help of software to realize the advanced control strategy.

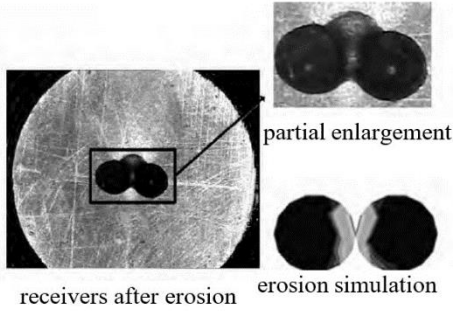


Fig. 2 Erosion of the pilot stage [13]

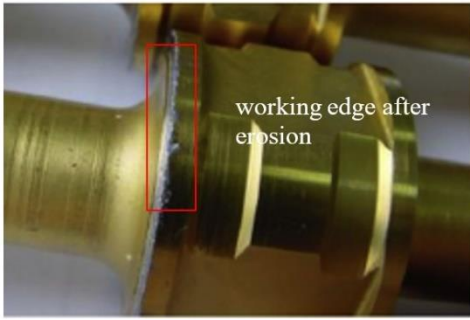


Fig. 3 Erosion of the slide valve stage

The unbalanced barrel pitching system is a complex position control system, the key of electro-hydraulic position control is to suppress the internal and external interference of which [15]. As a typical electrohydraulic coupling system, the control task shown in Fig. 4 is mainly to suppress the influence of erosion and other interference factors. The existing position control strategies can be divided into classical, modern and intelligent control technologies. In the classical control technology, PID has the advantage of simple structure, strong robustness and easy engineering, but it can not achieve good control effect for time varying uncertainty and strong interference systems. In intelligent control technology, sliding mode control is not affected by the parameters of the control object and the operating environment, especially for time-varying uncertain systems, it has good control accuracy and performance, but sliding mode control has special requirements for the amplitude of external interference and is prone to chattering; Therefore, neural network approximation is used to realize the adaptive approximation of unknown model such as interference, and good control effect is achieved. In other words, a single control method has its own defects, and the integration of two or more control algorithms can make up for the shortcomings and improve the control performance.

Firstly, this paper establishes the pressure and position double loop state space model of unbalanced barrel pitching system in part 2. Secondly, the erosion behavior

mechanism model of jet pipe servo valve is constructed, and the performance degradation characteristics of unbalanced barrel pitching control system under the condition of erosion are analyzed in part 3. According to the actual double loop structure characteristics of internal pressure loop and external position loop, the compound controller of inner loop PID and outer loop RBF-SMC is designed for compensation control of the unbalanced barrel pitching system.

2. Barrel pitching system' s dynamic model

The structural diagram of barrel pitching system is shown as Fig. 4, the unbalanced barrel is installed on the carrier platform and the barrel pitching control drive adopts the form of jet pipe servo valve driving hydraulic cylinder. The pitching angle of the barrel relative to the carrier is θ , which is measured using the attitude sensor and the pressure difference between the two chambers of the hydraulic cylinder is measured using the pressure difference sensor, all of which are sent to the system controller in real time. The control voltage is calculated by the control algorithm and sent to the jet pipe servo valve through the servo amplifier. By changing the size and direction of the current entering the servo valve, the pressure difference between the two chambers can be adjusted to realize the pitching control of the barrel.

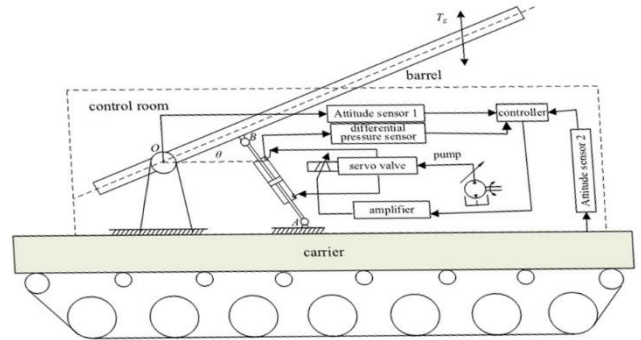


Fig. 4 The unbalanced barrel pitching control system

The servo amplifier can convert control voltage $U_1(t)$ into control current $I(t)$ so as to control the jet pipe servo valve, so the mathematical model of which can be expressed as:

$$K_a = \frac{I(t)}{U_1(t)}. \quad (1)$$

The natural frequency of each assembly inside the jet pipe servo valve is much higher than the barrel pitching frequency, so the relationship model between the power stage spool displacement $x_v(t)$ and the control current $I(t)$ can be expressed as:

$$K_1 = \frac{x_v(t)}{I(t)}. \quad (2)$$

The pilot stage's erosion shown in Fig. 2 will induce the increase of distance between the nozzle receiver and finally affect the value of K_1 .

The relationship between power stage spool displacement $x_v(t)$ and load flow $Q_l(t)$ can be expressed as:

$$Q_f(t) = k_q x_v(t) - k_c p_f(t), \quad (3)$$

where: $p_f(t)$ is the pressure difference between the two chambers of the hydraulic cylinder; k_q is the flow gain of the power stage slide valve; k_c is the pressure flow gain of the power stage slide valve. In Fig.3, the erosion power stage will affect the values of k_q and k_c .

With the aid of hydraulic oil source, the servo valve outputs the flow with adjustable size and direction to the double chamber of hydraulic cylinder. Ignoring the small return oil pressure, the continuous flow equation from the oil

source to the hydraulic cylinder can be expressed as:

$$Q_f(t) - C_l p_f(t) = A \frac{dl(t)}{dt} + \frac{v_0}{\beta_e} \frac{dp_f(t)}{dt}, \quad (4)$$

where: C_l is the leakage coefficient; A is the effective area of the piston cylinder in the hydraulic cylinder; V_0 is the single chamber volume of the hydraulic cylinder; β_e is the effective volume elastic model.

Since the final control variable of the system is the pitching angle of the barrel, so Eq. (4) is converted to Eq. (5).

$$\frac{dl(t)}{dt} = \frac{l_1(t)l_2(t)\sin(\gamma+\theta(t))}{\sqrt{l_1^2(t)+l_2^2(t)-2l_1(t)l_2(t)\cos(\gamma+\theta(t))}} \frac{d\theta(t)}{dt}. \quad (5)$$

In Eq. (5), let:

$$L(\theta) = \frac{l_1(t)l_2(t)\sin(\gamma+\theta(t))}{\sqrt{l_1^2(t)+l_2^2(t)-2l_1(t)l_2(t)\cos(\gamma+\theta(t))}}. \quad (6)$$

The torque balance equation between hydraulic cylinder and load can be expressed as:

$$M(t) = J \frac{d^2\theta(t)}{dt^2} + B_m \frac{d\theta(t)}{dt} + G\theta(t) + T_g(\theta), \quad (7)$$

where: J is the inertia of the barrel relative to the trunnion; B_m is the viscous damping coefficient; G is the load elastic stiffness; $T_g(\theta)$ is the unbalanced torque of the barrel.

The output torque $M(t)$ of the hydraulic cylinder is expressed as the product of the output force and the force arm as:

$$M(t) = p_f(t)AL(\theta). \quad (8)$$

By Laplace transformation and simultaneous solution of Eqs. (1) ~ (8), the relationship between the angle of barrel relative to carrier and control voltage and unbalanced torque can be obtained as follows:

$$\theta(t) = \frac{ALK_a K_1 k_q U_1(t) - \left(\frac{v_0}{\beta_e} s + k_c + C_l \right) T_g(t)}{\frac{v_0 J}{\beta_e} s^3 + \left(\frac{v_0 B_m}{\beta_e} + k_c J + C_l J \right) s^2 + \left(A^2 L^2 + k_c B_m + C_l B_m \right) s}. \quad (9)$$

From Eq. (9), It can be obtained the unbalanced barrel pitching system is a third order system. In order to improve the control effect, taking $p_f(t)$ as the intermediate variable, the whole system is divided into internal and external control structures. That is in the pressure inner loop, taking $x_1=p_f(t)$ and x_2 as the derivative of $p_f(t)$, then the state space model of the pressure inner loop can be obtained based on formulas (1) - (7):

$$\begin{cases} y = x_1(t) \\ \dot{x}_1(t) = x_2(t) \\ \dot{x}_2(t) = f_\theta(x) + g_\theta(u)u + d_\theta(t) \end{cases}, \quad (10)$$

$$\text{where: } f(x) = -\frac{(k_c + C_l)\beta_e}{v_0} x, \quad g(u) = \frac{\beta_e k_q K_1 K_a}{v_0},$$

$$u = U_1(t), \quad d(t) = -AL(\theta) \frac{\beta_e}{v_0} \frac{d\theta(t)}{dt}.$$

Furthermore, the state space model of the position outer loop can be obtained based on Eqs. (7) and (8), which is shown as:

$$\begin{cases} y = x_1(t) \\ \dot{x}_1(t) = x_2(t) \\ \dot{x}_2(t) = f_\theta(x) + g_\theta(u)u + d_\theta(t) \end{cases}, \quad (11)$$

$$\text{where: } f(x) = -\frac{G}{J} x_1 - \frac{B_m}{J} x_2, \quad g(u) = \frac{AL(\theta)}{J} u,$$

$$u = p_f(t), \quad d(t) = -\frac{T_g(t)}{J}.$$

3. Analysis of failure

3.1. Erosion mechanism

Jet pipe servo valve is a high-precision flow control hydraulic element. In the process of production and use, it will inevitably produce solid particles and other pollutants, which flow with the oil at a certain speed and angle in the internal flow channel, resulting in the erosion on the inner surface of the flow channel, mainly including the jet pipe amplifier of the pilot stage and the throttling edge of the power stage.

3.1.1. Jet amplifier of the pilot stage

Fig. 5 is the schematic diagram of the pilot stage nozzle receivers' erosion. The nozzle sprays high speed oil containing contaminated particles to the receivers, resulting in serious erosion at the receiver wedge and increasing the distance between the nozzle and the receivers.

Due to the complex flow field in the jet pipe amplifier, the flow equation is mainly established by theoretical formula combined with experimental verification. Some experimental studies have verified that when working in a small range, the comprehensive characteristics of the jet pipe amplifier is a straight line, and its equation can be expressed as Eq. (12).

$$q_j(t) = K_j x_j(t) - K_{cj} p_j(t), \quad (12)$$

where: $p_j(t)$ is the pressure difference between two chambers of valve core; K_j is the flow gain of the jet pipe amplifier; $x_j(t)$ is the displacement of the jet nozzle; K_{cj} is the pressure flow gain of the jet pipe amplifier.

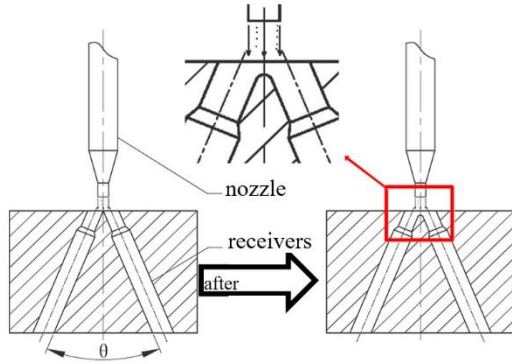


Fig. 5 Schematic diagram of receivers' erosion [13]

K_j and K_{jc} are all affected by the oil supply pressure, oil return pressure, nozzle diameter, receiver diameter, distance between nozzle and receivers, angle between two receivers and other factors of the jet pipe servo valve. In this paper, the determined servo valve is selected, and the flow equation is mainly affected by the distance between nozzle receivers. Fig. 6 shows the receiving area model of jet amplifier, the calculation of the coverage positioning angles θ_1 , α_1 , θ_2 , α_2 is shown as Eqs. (13)-(16).

$$\theta_1 = \arccos \left(\frac{R^2 + (R+L+x_j)^2 - r^2}{2R(R+L+x_j)} \right), \quad (13)$$

$$p_v(t) = \frac{1}{2} \rho \left(\frac{f_1 - f_2}{f_n \cos \alpha} \right) \sigma \left[C_d^2 \frac{2}{\rho} \frac{f_0^2}{f_n^2 + f_0^2} (p_s - p_t) + 2g \left(e + \frac{1}{2} r_0 \theta_j^2 \right) \right], \quad (19)$$

$$q_v(t) = \left(\frac{f_1 - f_2}{f_n \cos \alpha} \right) \sqrt{C_d^2 \frac{2}{\rho} \frac{f_0^2}{f_n^2 + f_0^2} (p_s - p_t) + 2g \left(e + \frac{1}{2} r_0 \theta_j^2 \right)}. \quad (20)$$

where: ρ is the oil density; e is the distance between the nozzle and the receiver; f_n is the nozzle area; σ is the loss coefficient; p_s is the supply pressure; p_t is the return pressure; θ

$$\alpha_1 = \arccos \left(\frac{r^2 + (R+L+x_j)^2 - R^2}{2r(R+L+x_j)} \right), \quad (14)$$

$$\theta_2 = \arccos \left(\frac{R^2 + (R+L-x_j)^2 - r^2}{2R(R+L-x_j)} \right), \quad (15)$$

$$\alpha_2 = \arccos \left(\frac{r^2 + (R+L-x_j)^2 - R^2}{2r(R+L-x_j)} \right), \quad (16)$$

where: R and r are respectively the diameter of the receiver and nozzle; L is the edge width between receivers; the initial value of L is 0, but with the progress of erosion; L will gradually increase; x_j is the nozzle displacement.

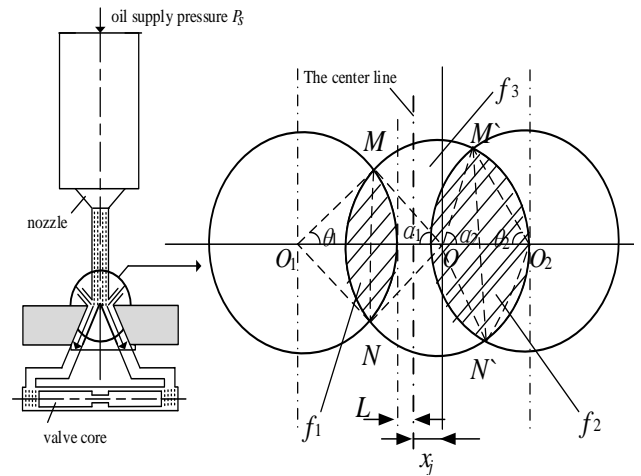


Fig. 6 The receiving area model of the jet amplifier

The areas f_1 and f_2 of the nozzle covering the left and right receiving holes are:

$$f_1 = R^2 \theta_1 + r^2 \alpha_1 - \sin(\theta_1) R (R+L+x_j), \quad (17)$$

$$f_2 = R^2 \theta_2 + r^2 \alpha_2 - \sin(\theta_2) R (R+L-x_j). \quad (18)$$

Based on the energy conservation, the load pressure and load flow of the jet amplifier can be deduced as Eqs. (19) and (20) respectively.

is the nozzle's offset angle; C_d is the nozzle's flow coefficient.

As shown in Fig. 7, the initial distance between the

nozzle and the receiver is e , and the increase of the distance between the nozzle and receiver induced by erosion is L_e , so the relationship between the wedge size and the increase of the erosion distance is shown as Eq. (21).

$$L = L_e \tan\left(\frac{\alpha}{2}\right). \quad (21)$$

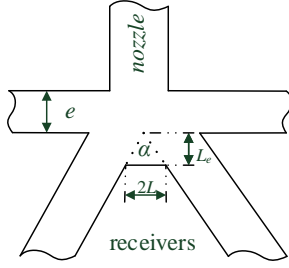


Fig. 7 The relationship between wedge width and erosion amount

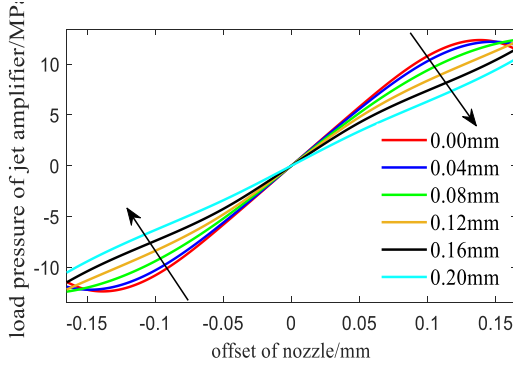


Fig. 8 Pressure characteristics of jet amplifier under different erosion

The distance between nozzle and receivers increases gradually with the progress of erosion, and the

$$Q_f(t) = C_v W \sqrt{\frac{1}{\rho}} \left((x_0 + x_v(t)) \sqrt{p_s - p_f(t)} - ((x_0 - x_v(t)) \sqrt{p_s + p_f(t)}) \right). \quad (22)$$

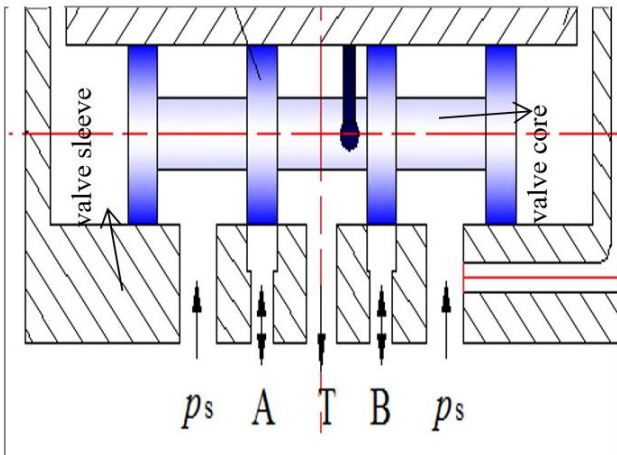


Fig. 10 The structure diagram of the valve core and valve sleeve

The valve core often works around the zero position, so let $x_v(t)$, $Q_f(t)$ and $p_f(t)$ are all 0. The linearization of Eq. (22) of is as follows:

wedge width will also increases. Which will eventually cause the changes of the jet amplifier's characteristics. In order to quantitatively explore the performance degradation law of the pilot stage induced by erosion, the performance curves under different erosion quantities are calculated and fitted shown as Figs. 8 and 9.

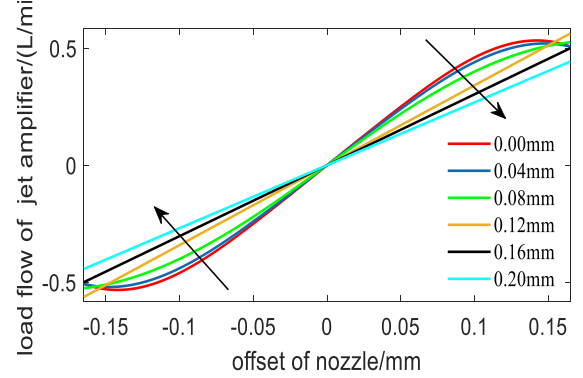


Fig. 9 Flow characteristics of jet amplifier under different erosion

3.1.2. Throttling edge of the power stage

The structure diagram of the valve core and valve sleeve of jet pipe servo valve's power stage is shown as Fig. 10. The nozzle deflection of the pilot stage causes the pressure of the two receiving holes to be no longer balanced, and the pressure difference between the left and right chambers drives the valve core to move. The movement of the valve core causes the change of the relative position between the valve core and valve sleeve, so as to realize the control of the on-off of the oil port. In fact, due to erosion, the throttling edge's fillet of the valve core and valve sleeve will increase.

The power stage slide valve of jet pipe servo valve adopts the structural form of three position four-way, and the load flow calculation is shown as Eq. (22).

$$Q_f(t) = \frac{\partial Q_f(t)}{\partial x_v(t)} x_v(t) + \frac{\partial p_f(t)}{\partial p_f(t)} p_f(t) = k_q x_v(t) - k_c p_f(t), \quad (23)$$

where: $Q_f(t)$ is the load flow of the spool; $p_f(t)$ is the load pressure of the spool; k_q is the flow gain of the spool; k_c is the pressure flow gain of the spool.

The calculation of k_q and k_c are as Eqs. (24) and (25).

$$k_q = C_v W \sqrt{\frac{1}{\rho}} p_s. \quad (24)$$

$$k_c = \frac{\pi W \Delta^2}{32 \mu}. \quad (25)$$

As shown in Fig. 11, the fillet radius R_w of the throttling edge will increase because of erosion, which in-

increases the equivalent opening when the valve core displacement x_v is the same as that before erosion, and finally leads to the change of flow pressure characteristics of the power stage.

$$L_w = 2R_w(2\sin(\alpha)-1) + \sqrt{(x_0 + x_v)^2 + \Delta^2}, \quad (26)$$

where: $L_{ax} = \frac{L_w \sin(\alpha)}{2}$.

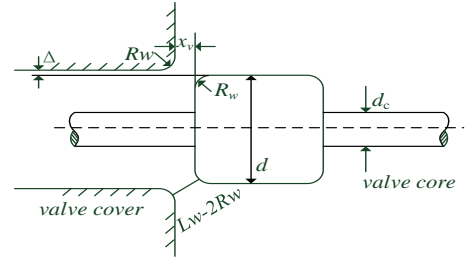


Fig. 11 The orifice model of spool valve

Then the flow gain and flow pressure gain of the spool valve after erosion are calculated as Eqs. (27) and (28) respectively.

$$k_{qe} = C_v \pi \sqrt{\frac{1}{\rho} p_s} \left(2R_w(2\sin(\alpha)-1)\sin(\alpha) + \sqrt{(x_0 + x_v)^2 + \Delta^2} \sin(\alpha) + d \right), \quad (27)$$

$$k_{ce} = \frac{\pi^2 \left(2R_w(2\sin(\alpha)-1)\sin(\alpha) + \sqrt{(x_0 + x_v)^2 + \Delta^2} \sin(\alpha) + d \right) \Delta^2}{32\mu}, \quad (28)$$

where: d is the diameter of the valve core.

Based on Eqs. (27) and (28), the flow gain and flow pressure gain under different erosion fillet and spool displacement are calculated. The change trends of flow gain and flow pressure gain can be obtained by multi group calculation analysis and data fitting are shown as in Figs. 12 and 13 respectively.

From Fig. 12, it can be obtained the flow gain increases monotonically with the erosion fillet and spool displacement, but it is more affected by the spool displacement. When the spool displacement is 0, the flow gain value is not the initial value of 0. With the extension of service time, the erosion fillet gradually increases and the valve core displacement takes a cyclic value between 0 and the maximum displacement value. Therefore, it is necessary to take a average value of the flow gain corresponding to different displacement under a certain erosion fillet.

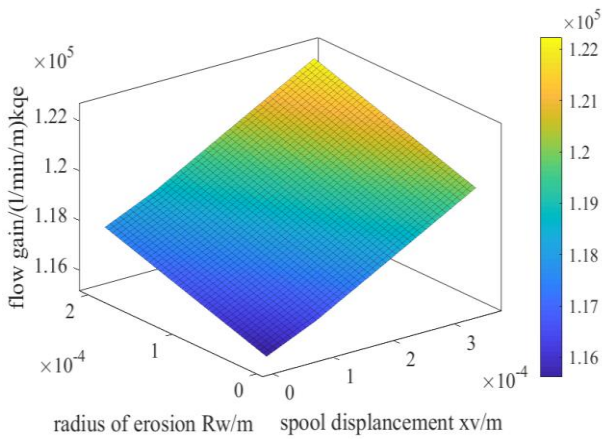


Fig. 12 The relationship between flow gain and erosion radius and spool displacement

In Fig. 13, the flow pressure gain follows the same law with the erosion fillet and spool displacement, that is, which increases monotonically with the erosion fillet and spool displacement and is more affected by the spool displacement, but the change gradient of flow pressure gain is larger than that of flow gain. When the spool displacement is 0, the value of pressure flow gain is not the initial value

of 0. With the extension of service time, the erosion fillet gradually increases, but the valve core displacement takes a circular value between 0 and the maximum value. Therefore, it is necessary to take a average pressure flow gain corresponding to different displacements under a certain erosion fillet.

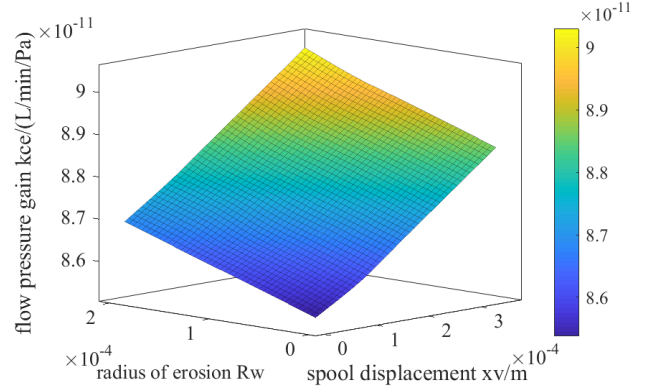


Fig. 13 The relationship between pressure flow gain and erosion radius and spool displacement

3.2. Numerical calculation

Based on CFD theory and erosion theory, Reynolds averaged Navier-Stokes equation, standard $k-\varepsilon$ two equation model, discrete phase flow model and plastic material erosion model are used to simulate the erosion of the nozzle receiver of the pilot stage and the throttling edge of the power stage. The distribution of erosion rate is predicted by FLUENT software, and the high speed oil is taken as a continuous phase to simulate its flow field in Euler coordinates. Take the particles in the oil as discrete phase to calculate their motion orbit in Lagrangian coordinates. Select the probability distribution function to solve the velocity and angle information of solid particles, and then calculate the distribution of erosion rate with a quantitative model. This process needs to complete three aspects: internal flow field calculation, solid particle orbit calculation and erosion rate calculation.

A certain distance from the front end of nozzle to

the rear end of the receiving hole is selected as the numerical simulation range. In order to accurately obtain the distribution of erosion rate on the inner wall of the nozzle receiver, a calculation model of the erosion rate is established, shown as Fig. 14. Similarly, the erosion calculation model of power stage is established as Fig. 15.

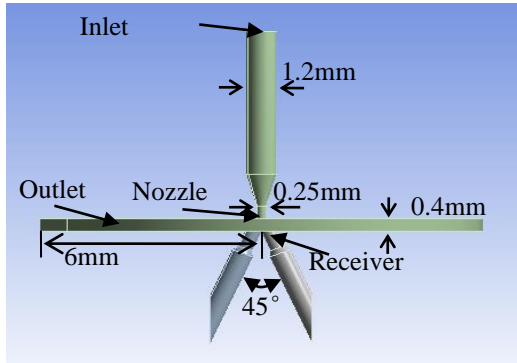


Fig. 14 The erosion simulation model of the pilot stage

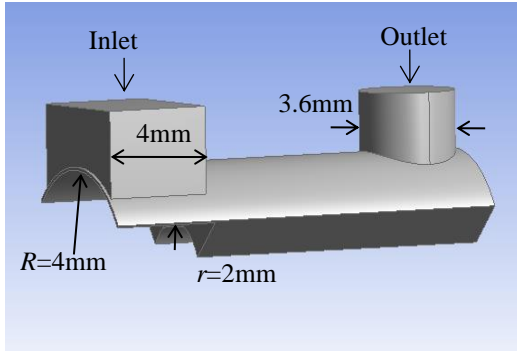


Fig. 15 The erosion simulation model of the power stage

The flow field of the pilot stage from nozzle to receiver is the most complex, the mesh division of which is encrypted to improve the accuracy of the simulation. The hydraulic oil with oil density of 855 kg/m^3 and dynamic viscosity of $0.01254 \text{ Pa}\cdot\text{s}$ is selected as the working medium. The boundary condition of pressure inlet and pressure outlet are set as 21 MPa and 0.5 MPa respectively, and the residual convergence accuracy is set as 10^{-5} . The discrete phase model is set to simulate the particle trajectory and calculate the erosion rate. The oil inlet is set as the injection plane of contaminated particles. The DRW model is selected to deal with the interaction between particles and fluid discrete vortices. The velocity distribution and erosion rate distribution of the pilot stage are obtained by running the numerical simulation program shown as Figs. 16 and 17 respectively.

Fig. 16 shows the velocity at the front end of the nozzle is small and evenly distributed. With the contraction of the nozzle size, the jet velocity increases rapidly and reaches the maximum velocity of 202 m/s , then the jet velocity will gradually decrease due to entering the receiving holes with increased size. It is worth noting that the liquid flow will also form a slightly higher reflux velocity when touching the receiver wedge.

The high speed flowing oil is mixed with contaminated particles, most of the particles enter the receiving holes through the jet nozzle, return with the oil and finally flow out of the outlet of the disc. Based on the velocity distribution and particle trajectory, it is easy to know that the erosion rate at the wedge of the receiving hole is relatively

the largest shown as Fig. 17, in which the erosion rate distribution gradually decreases from the center of the wedge to both sides.

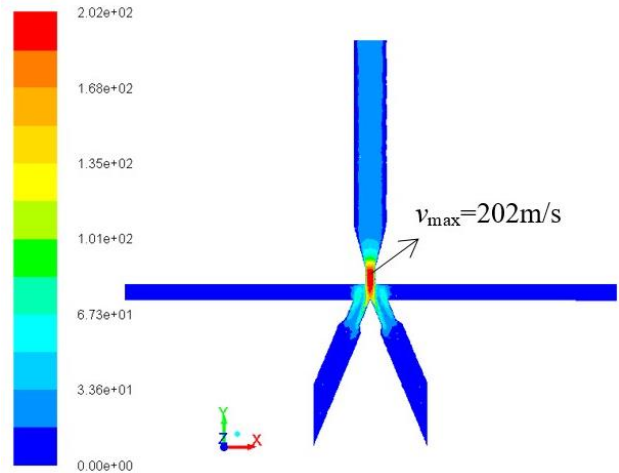


Fig. 16 The velocity distribution of the pilot stage

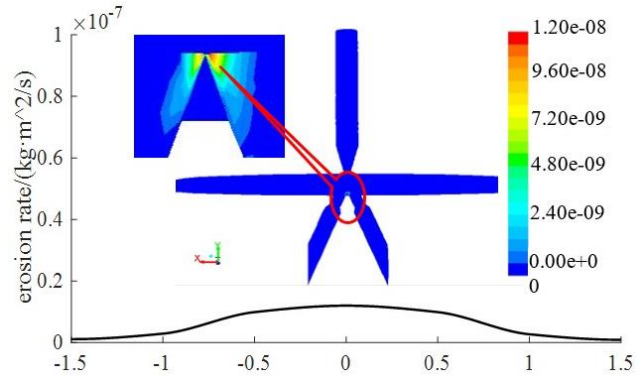


Fig. 17 The erosion rate distribution of the pilot stage

Similarly, the velocity distribution and erosion rate distribution of power stage obtained by numerical simulation are shown as Figs. 18 and 19 respectively. The oil mixed with contaminated particles enters from the inlet, and the speed increases significantly to 155 m/s at the throttling edge. Then after entering the wide area between the valve core and valve sleeve, the speed decreases gradually and finally flows out from the outlet. The contaminated particles will have a greater erosion effect on the throttling edge with the oil, and the greater the distance away from the edge, the smaller the erosion rate as shown in Fig. 19.

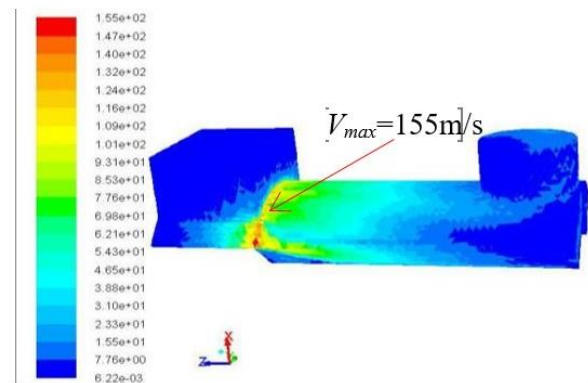


Fig. 18 The velocity distribution of the power stage

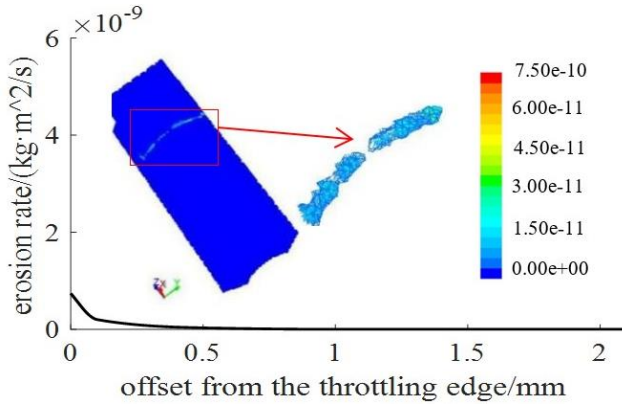


Fig. 19 The erosion rate distribution of the power stage

3.3. Characteristics degradation of barrel pitching system

In order to explore the performance degradation degree of barrel pitching system induced by gradual erosion behavior, the simulation model of barrel pitching system is built based on the system mathematical model. The barrel rotation command of 0.524 rad (30°) is input, the barrel pitching response without erosion wear, 0.2 mm erosion distance of pilot stage and 180 um erosion fillet radius of power stage are analyzed as Fig. 20. It can be found that the erosion of pilot stage and power stage will all cause the deterioration of the barrel control performance, which is mainly reflected in the attenuation of the barrel stable displacement under the same control command. However, which has little effect on the dynamic performance of the barrel. In contrast, the performance degradation induced by erosion of the pilot stage is higher than that of the power stage. Therefore, effective control strategies need to be researched in order to compensate control the performance degradation caused by erosion.

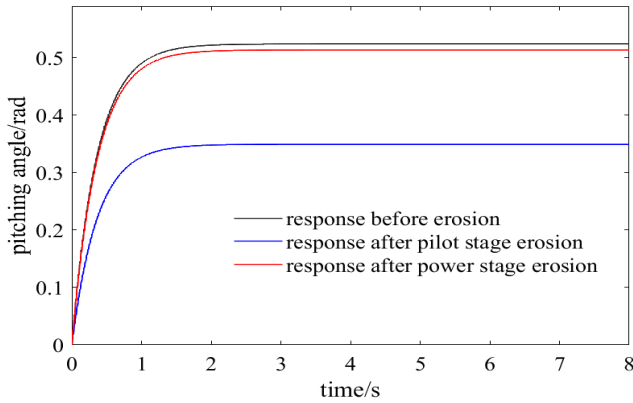


Fig. 20 The contrast of the barrel pitching response under erosion

4. The compensation control for the characteristics degradation of barrel pitching

4.1. Design of pressure-position double loop controller

The control block diagram of the unbalanced barrel pitching system is shown as Fig. 21. The jet pipe servo valve is used to control the hydraulic cylinder to realize the pitching drive of the barrel. The oil pressure sensor and high precision attitude sensor are used to collect the double chamber pressure difference of the cylinder and the barrel pitching

angle in real time, form the pressure feedback inner loop and position feedback outer loop respectively. The RBFNARSM-PID two-stage controller is designed to compensate the deterioration of internal structural parameters induced by erosion, and finally realize the high performance control of barrel pitching under the given control command.

The part marked in red in Fig. 21 is the position pressure double loop composite controller, which is composed of RBF Network Adaptive Robust Sliding Mode and Proportional Integral Derivative controller. Among them, the internal pressure loop adopts PID control, while the outer loop adopts RBFNARSMC control.

The internal PID control algorithm is:

$$u(t) = k_p e_p(t) + k_i \int_0^t e_p(t) + k_d \frac{de_p(t)}{dt}. \quad (29)$$

The external is RBF network adaptive robust sliding mode control algorithm, in which the input and output algorithm of RBF network is:

$$h_j = \exp\left(-\frac{\|x - c_j\|^2}{2b_j^2}\right), \quad (30)$$

$$f(\bullet) = W^{*T} h_f(x) + \varepsilon_f, \quad (31)$$

$$g(\bullet) = V^{*T} h_g(x) + \varepsilon_g, \quad (32)$$

where: x is the network input; i is the i th input of the network input layer; j is the j th network input of the network hidden layer; $h = [h_j]^T$ is the output of the Gaussian basis function; W^* and V^* are the ideal network weights of the approximation to f and g , and ε_f and ε_g are the network approximation error.

The output of RBF is:

$$\tilde{f}(x) = \tilde{W}^T + h_{gf}(x), \quad \tilde{g}(x) = \tilde{V}^T + h_g(x). \quad (33)$$

The control law is designed as:

$$u_\theta(t) = \frac{1}{\tilde{g}(x)} \left[-\tilde{f}(x) \right] + \ddot{\theta}_d + c e_\theta + \eta \text{sgn}(s). \quad (34)$$

4.2. The construction of barrel pitching experimental system

In order to verify the effectiveness of the barrel pitching compensation control method, an unbalanced barrel pitching experimental system considering the impact of erosion is built. The control system adopts STM32 for high precision compensation control of barrel pitching, which includes measuring the attitude angle of barrel and the pressure of hydraulic cylinder in real time, calculating the control voltage of jet pipe servo valve based on the control algorithm, and finally completing the control of barrel pitching angle. The detailed composition of the barrel pitching control experimental system is shown as Fig. 22.

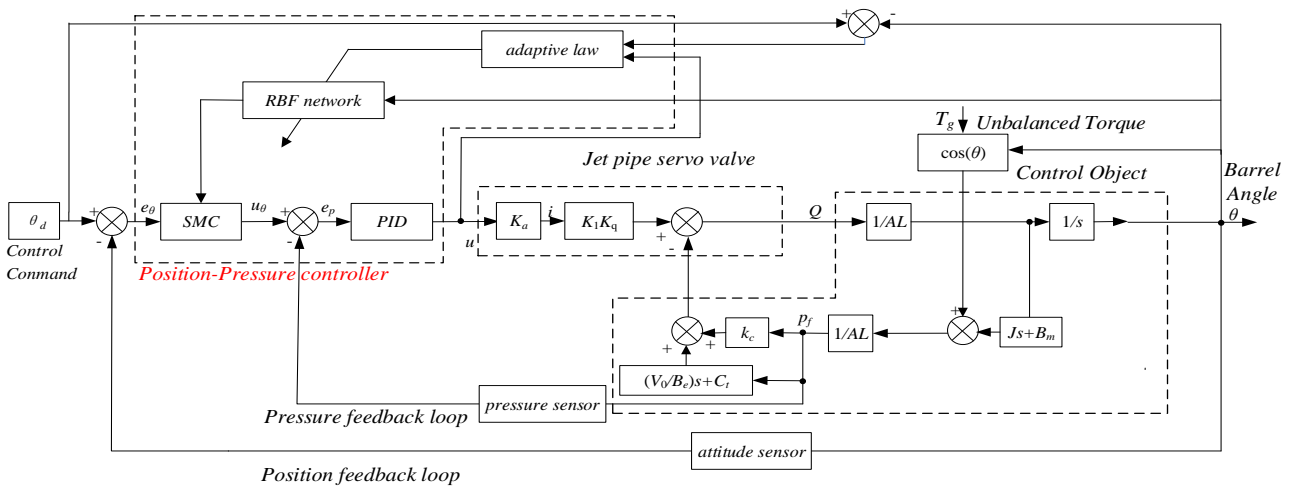


Fig. 21 Design of pressure-position double loop controller

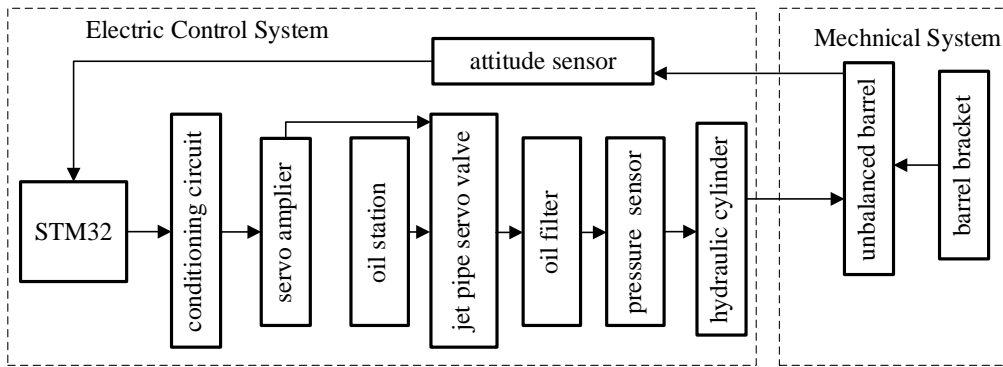


Fig. 22 The detailed composition of the barrel pitching control experimental system

4.3. Results and discussion

1. The comparison of related algorithms' control effect.

Under the initial conditions, SMC, PID and SMC+PID algorithms are selected to control the unbalanced barrel pitching system. The step command with amplitude of 0.524 rad (30°) is used as input, then the barrel pitching angle response is shown in Fig. 23. After comparison, it can be found the barrel pitching response under SMC control has the best rapidity, but there is an overshoot that can not be ignored, and there is a certain error in the stable angle.

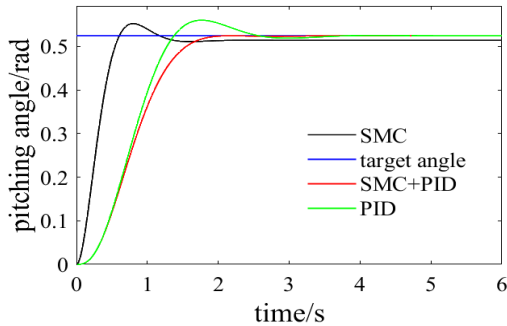


Fig. 23 The contrast of barrel pitching control

The steady state error of PID control can reach the allowable range, but its dynamic adjustment time is more than 3s. Although the rise time of SMC+PID composite control is longer than the others, there is no overshoot and the stability time is only 2s, and the steady state error achieves

a satisfactory control result in a short time. Therefore, SMC+PID compound control is relatively more suitable for the effective control of unbalanced barrel pitching system.

2. The compensation control of the erosion influence.

After erosion, the performance of barrel pitching system will inevitably deteriorate. The performance degradation includes two inducements: the erosion of the pilot stage and the power stage. The numerical analysis results of erosion show that the erosion rate of the two position are different. In order to effectively compensate and control the system performance degradation, the erosion amount at different time points is calculated based on the standard of time. Then the corresponding deterioration parameters are obtained and brought into the barrel pitching system to determine the compensation control effect. Fig. 24 shows the comparison of system compensation control effect under different service time. It can be found that with 0.524 rad (30°) step input, after SMC+PID compound control, the barrel pitching response is different, but the difference is small, that is, the dynamic and steady state performance have been effectively compensated.

Fig. 25 shows the comparison of system compensation control effect under different service time. It can be found that under the sinusoidal target angle of 0.524 rad (30°), after SMC+PID compound control, the difference of barrel pitching sinusoidal tracking response is small, that is, the dynamic and steady state performance of the compensation control system is good.

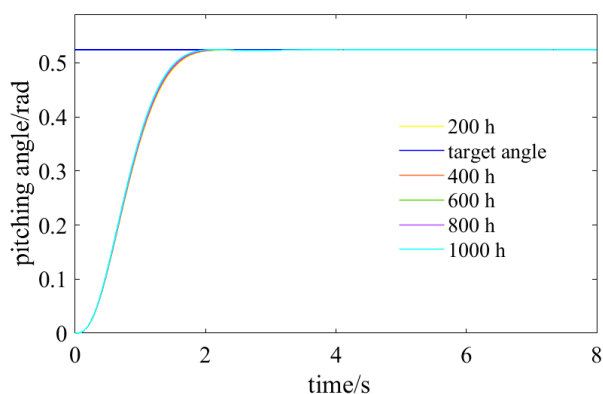


Fig. 24 Barrel pitching step response under erosion

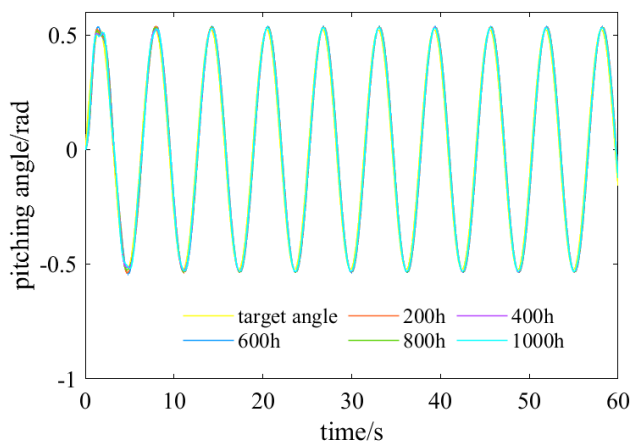


Fig. 25 Barrel pitching sinusoidal track response under erosion

3. The barrel pitching control experiment. When the service time of barrel pitching system is 1000 hours, the steady state performance deteriorates. The inducement includes the change of pilot stage's flow gain, the power stage's flow gain and pressure flow gain. The barrel pitching experimental system is built, and the system controller is designed based on SMC+PID composite control algorithm. The step barrel turning command and sinusoidal tracking command with the amplitude of 200 mil are given respectively, and the barrel pitching step response and sinusoidal tracking response are obtained as Figs. 26 and 27 respectively.

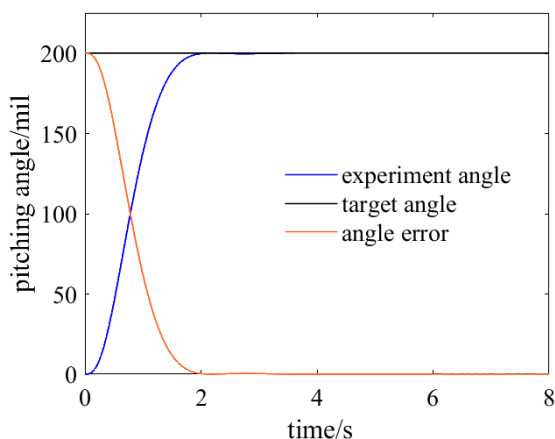


Fig. 26 The barrel pitching step response

In Fig. 26, after receiving the step command, the barrel enters a stable state without overshoot in about 2 s,

and the stability error less than 1.6 mil meets the system requirements. In the sinusoidal tracking response shown as Fig. 27, the target command can be tracked by quickly adjusting the barrel pitching angle in the first quarter cycle, and the tracking error fluctuates around 5.6 mil. Experiments show that SMC+PID control method can effectively compensate the performance degradation of barrel pitching system.

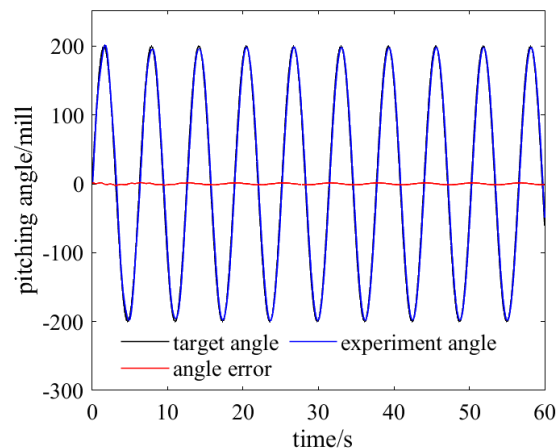


Fig. 27 The barrel pitching sinusoidal tracking response

5. Conclusion

As the core of barrel pitching system, jet pipe servo valve is a complex high precision electrohydraulic servo component. In the service process of barrel weapons, the jet pipe servo valve will inevitably occur erosion behavior, which will induce the changes of pilot stage's flow gain, power stage's flow gain and pressure flow gain, resulting in the deterioration of the servo valve's performance, and then the decline of the steady state performance of barrel pitching system. In order to improve the control performance, SMC+PID double loop algorithm is designed for the compensation control of barrel pitching system. The inner loop takes the hydraulic cylinder pressure difference as the control variable, uses PID controller for pressure stability control, and the outer loop uses RBF network adaptive sliding mode controller for barrel pitching angle control. Through software simulation and experimental verification, it is found the given control algorithm can realize the compensation control of barrel pitching system within limited service time, and the dynamic and stable control performance can meet the needs of practical engineering.

References

1. Wang, C. M.; Xia, Y. Q.; Fu, M. Y. 2014. Application of active disturbance rejection control in tank gun control system, *Journal of the Franklin Institute* 351(4): 2299-2314. <https://doi.org/10.1016/j.jfranklin.2013.02.003>.
2. Rahman, A.H.; Malik, S.A.; Kumar, J. R. 2018. A design of experiments methodology for evaluating configuration for a generation next main battle tank, *Defence Science Journal* 68(1): 19-25. <http://doi.org/10.14429/dsj.68.12182>.
3. Yao, J. Y.; Deng W. X. 2017. Active disturbance rejection adaptive control of hydraulic servo systems. *IEEE Transactions on Industrial Electronics* 64(10): 8023-8032.

- <http://doi.org/10.1109/TIE.2017.2694382>.
4. **Yao, J. Y.; Deng, W. X.; Sun W. C.** 2017. Precision motion control for electro-hydraulic servo systems with noise alleviation: a desired compensation adaptive approach, *IEEE Transactions on Mechatronics* 22(4): 1859-1868.
<http://doi.org/10.1109/TMECH.2017.2688353>.
 5. **Yang, G. C.; Yao, J. Y.; Le, G. G.** 2016. Asymptotic output tracking control of electro-hydraulic systems with unmatched disturbances, *IET Control Theory & Applications* 10(18): 2543-2551.
<http://doi.org/10.1049/iet-cta.2016.0702>.
 6. **Yao, J. Y.; Deng, W.X.; Jiao Z. X.** 2017. RISE-based adaptive control of hydraulic systems with asymptotic tracking, *IEEE Transactions on Automation Science and Engineering* 14(3): 1524-1531.
<http://doi.org/10.1109/TASE.2015.2434393>.
 7. **Liu, J. C.; Jayakumar P.** 2017. A nonlinear model predictive control formulation for obstacle avoidance in high-speed autonomous ground vehicles in unstructured environments, *Vehicle System Dynamics* 55(10): 1-30.
<http://doi.org/10.1080/00423114.2017.1399209>.
 8. **Vantsevich, V.; Paldan, J.; Farley B.** 2016. Mobility optimization and control of a 4x4 he-vehicle in curvilinear motion on stochastic terrain, *Proceedings of the ASME 2016 International Design Engineering Technical Conferences and Computers and Information in Engineering Conference*, New York: ASME, p. 1-10.
 9. **Zhang, K.; Yao, J. Y.; Jiang T. M.** 2014. Degradation assessment and life prediction of electro-hydraulic servo valve under erosion wear, *Engineering Failure Analysis* 36(1): 284-300.
<http://doi.org/10.1016/j.engfailanal.2013.10.017>.
 10. **Yao, J. Y.; Luo, R. M.; Yin X. Z.** 2014. Research on degradation behavior propagation model based on wear, *Reliability & Maintainability Symposium* 94(23): 1-7.
<http://doi.org/10.1109/RAMS.2014.6798439>.
 11. **Gao, Q.; Hou, Y. L.; Li K.** 2016. Neural network based active disturbance rejection control of a novel electro-hydraulic servo system for simultaneously balancing and positioning by isoactuation configuration, *Shock and Vibration* 23(9): 10-19.
<http://doi.org/10.1155/2016/4921095>.
 12. **Li, K.; Gao, Q.; Gong J.** 2015. Modeling and simulation of electro-hydraulic servo system of a certain weapon barrel for balancing and positioning, *27th Chinese Control and Decision Conference*, New York, IEEE, 3397-3401.
 13. **Yin, Y. B.; Fu, J. H.; Jin Y. L.** 2015. Numerical simulation of erosion wear of the pre-stage of the jet pipe servo valve, *Journal of Zhejiang University* 49(12): 2252-2260.
<http://doi.org/10.3785/j.issn.1008-973X.2015.12.003>.
 14. **Gao, Z. Q.** 2014. On the centrality of disturbance rejection in automatic control, *Isa Transactions* 53(4): 850-857.
<http://doi.org/10.1016/j.isatra.2013.09.012>.

Y. Chu, Y. Xia

THE INVESTIGATION OF A UNBALANCED BARREL PITCHING SYSTEM'S CHARACTERISTICS DEGRADATION AND COMPENSATION UNDER GRADUAL EROSION BEHAVIOR

S u m m a r y

The unbalanced barrel pitching system is a typical electro-hydraulic coupling servo control system, the performance of which determines the response speed and hit probability of vehicle mounted weapon equipment. However, in the actual service process, its core component, the high precision jet pipe servo valve, will produce the gradual erosion of the pilot stage's receivers and the power stage's throttling edges, which will induce the performance degradation of the unbalanced barrel pitching system, and finally greatly reduce the performance of barrel weapons. Therefore, a pressure and position double loop state space model of unbalanced barrel pitching system including the core parameters of performance degradation is established. The erosion behavior mechanism model of jet pipe servo valve is constructed, and the performance degradation characteristics of the unbalanced barrel pitching control system under the condition of erosion are further analyzed. Finally, aiming at the double loop structure of internal pressure loop and external position loop, the RBF Network Adaptive Robust Sliding Mode-Proportional Integral Derivative two-stage controller of barrel system is designed, based on which the experimental platform of unbalanced barrel pitching control is built. The experimental results are in good agreement with the theoretical results, so the proposed control method can effectively suppress the degradation of internal structural parameters induced by erosion, that is, it can better compensate the performance degradation of barrel pitching system induced by gradual erosion behavior.

Keywords: erosion wear, barrel pitching system, unbalance torque, jet pipe servo valve, sliding mode control.

Received August 30, 2022

Accepted April 5, 2023



This article is an Open Access article distributed under the terms and conditions of the Creative Commons Attribution 4.0 (CC BY 4.0) License (<http://creativecommons.org/licenses/by/4.0/>).